Dynamic Temperature Estimation of Power Electronics Systems

Pamela J. Tannous, Satya R. T. Peddada, James T. Allison, Thomas Foulkes, Robert P. Pilawa, and Andrew G. Alleyne*

***Abstract*— This paper proposes a method for accurate temperature estimation of thermally-aware power electronics systems. The duality between electrical systems and thermal systems was considered for thermal modeling. High dimensional thermal models present a challenge for online estimation. The complexity of the thermal network was reduced by applying a structure-preserving model order reduction technique. An optimal number of temperature sensors that increases the observability of the system was used in a Kalman filter to accurately estimate the dynamic spatial thermal behavior of the system.**

I. Introduction

With the emerging trend of increasing the power density of power electronics comes the limitation of the power dissipation in the system. The increase of power dissipation leads to an increase in temperature [1] that has negative effects on the performance and lifetime of the components operating in the power electronics system. Also, higher temperature increases the cooling cost which is a major problem in the current power electronics field [1]–[6]. Dynamic thermal management (DTM) was proven to be an effective solution to control the temperature by guaranteeing that the temperature of the hotspots in the system will not violate a specific threshold. However, this technique typically relies on thermal measurements obtained from on-board sensors. Therefore, accurate temperature readings of the system are essential for a successful DTM [7]–[9]. Power electronic systems that estimate their own temperature to apply thermal management techniques are known by thermally aware power electronics [5]. Increasing the power density becomes safer in this new breed of power electronic systems since the availability of the accurate dynamic temperature profile in these systems activates the DTM at the right time. Accurate thermal readings can be obtained easily by increasing the number of sensors in the system. However, a large number of sensors influences the reliability and packaging of the system, increases its cost, and interferes with its circuit design [7]. Furthermore, the locations of the temperature sensors in the system affect the accuracy of the estimated parameters.

*Research supported by the National Science Foundation Engineering Research Center for Power Optimization of Electro Thermal Systems (POETS) with cooperative agreement EEC-1449548.

P. J. Tannous (e-mail: tannous2@illinois.edu) and A. G. Alleyne (e-mail: alleyne@illinois.edu) are with the Mechanical Science and Engineering Department, University of Illinois at Urbana-Champaign, Urbana, IL 61801 USA (phone: 217-244-9993; fax: 217-244-6534).

Satya R. T. Peddada (email: speddad2@illinois.edu) and James T. Allison (email: jtalliso@illinois.edu) are with the Industrial and Enterprise Systems Engineering Department, University of Illinois at Urbana-Champaign, Urbana, IL 61801 USA (phone: 217-244-4319; fax: 217-244-5705).

Thomas Foulkes (email: foulkes2@illinois.edu) and Robert P. Pilawa (email: pilawa@illinois.edu) are with the Electrical and Computer Engineering Department, University of Illinois at Urbana-Champaign, Urbana, IL 61801 USA (phone: 217-244-0181).

The objective of this research is to obtain an accurate estimation of the spatial dynamic thermal profile of thermally aware power electronic systems using the smallest number of temperature sensors in the system. Current power electronic systems do not have the ability to extract the dynamic spatial temperature distribution of the system. Some work has been done on the temperature estimation for a single chip [7]. However, the method proposed in this paper provides a methodology for an accurate thermal estimation of highly complex and heterogeneous systems using an online model-based estimator and compact thermal models.

The rest of this article is organized as follows. Section II describes the thermal network modeling procedure. Section III describes the model order reduction technique used. Section IV describes the estimator design. Section V describes a case study in which the proposed method was tested on an actual multi-level inverter. Section VI presents the conclusion.

II. Thermal Network Modeling

A. RC modeling

The dynamic physical systems of interest have temporally and spatially varying temperature profiles. Detailed modeling of thermal interaction in these systems results in high dimension complex models that are inappropriate for estimation and control design purposes. The appropriate modeling approach needs to balance complexity versus accuracy. The thermal models should to be simple enough for on-line implementation and detailed enough to simulate the dynamic thermal behavior of the systems at an acceptable level of accuracy. Also, the number of powerful analysis tools drops significantly for non-linear systems compared to linear systems [10] leading to a strong preference for linear models. Therefore, the physical systems analyzed were approximated by lumped parameter models by deriving an equivalent thermal circuit [6]. Collecting these models results in a directed connected graph of linear systems. Model order reduction techniques can be used to further reduce the dimension of the lumped parameters models. This idea is detailed in Section III.

The first step towards getting an accurate temperature estimation of thermally-aware power electronic systems is to create a thermal model that provides an offline simulation of the dynamic thermal behavior of the system. In order to account for all the thermal effects in the system in full detail, numerical thermal analysis methods such as the finite element method must be used in the modeling procedure. However, these techniques result in complex high-dimensional models that are not suitable for estimation and control design purposes. Therefore, a tradeoff between accuracy and complexity must be done in order to obtain a thermal model that generates the dynamic thermal behavior of the system at

an acceptable level of accuracy with low computational efforts [2].

As shown in the literature, a resistor-capacitor (RC) thermal model can successfully simulate the spatial dynamic temperature distribution of the system with a reasonable accuracy and complexity tradeoff [2], [9], [11]–[13]. This thermal network is created by considering the similarity between an electric circuit and a thermal circuit since current and heat flow are described with the same differential equations. This similarity converts the heat conduction problem into an electric problem where the voltage in the RC circuit represents the temperature, the current represents the heat transfer, and the electrical resistances represent the thermal resistances. The capacitors used in the RC model simulate the transient behavior of the system by modeling the thermal lag that occurs before the temperature of the system reaches a steady state value following a change in the heat input.

The heat conduction problem can be solved as a 1D problem, 2D problem, or 3D problem [14]. For a 1D heat conduction problem, the system is divided into blocks along just one direction. The blocks are connected to each other through a thermal resistance. For a 2D heat conduction problem, the system is considered as a plate that is divided into pixels with an assigned capacitor to each one of these elements and assigned resistors that connect each capacitor to one other in the x and y directions. For a 3D heat conduction problem, the system is divided into small cubes, or voxels, with assigned resistors and capacitors that account for the conduction along three dimensions. Since dynamic thermal estimation requires computationally efficient thermal models, the level of granularity chosen for designing the thermal model of the power electronic systems was at the level of the functional elements [2]. Therefore, each functional block is represented by a single node and assigned a capacitor in the RC thermal model. The resulting RC model is characterized by a spatial correspondence with the physical system. Each capacitor in the RC model refers to a specific functional block in the physical system. The heat generated from the functional blocks is modeled as current sources connected to the corresponding capacitors in the RC model.

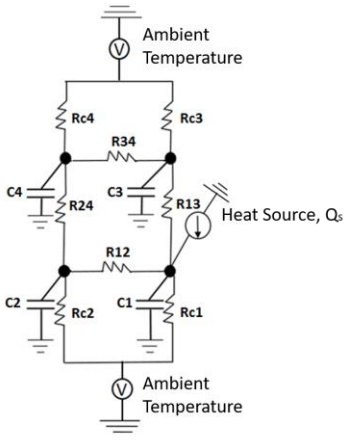

Fig.1. Example of a 2-D RC thermal model of a system that was partitioned into 4 pixels

The convection heat transfer from each functional block or each part of the system to the ambient temperature is represented in the RC model by a resistor that connects each relevant capacitor to the ambient temperature. The ambient temperature is represented in the RC model by a voltage source that allow the user to specify the specific ambient temperature that the system is subjected to. Fig.1 shows an example of a 2D RC circuit for a system divided into 4 elements. The heat generated in the first functional element was modeled by the current source connected to the first capacitor.

The next step in designing the thermal model is to compute the resistances and capacitors values. The conduction resistance is given by

$$R_{cond} = \frac{L}{KA_c}, \tag{1}$$

where L is the length through which the heat is being conducted, K is the thermal conductivity of the material, and A_c is the cross sectional area through which the heat is being conducted. The type of heat transfer from a surface of a system depends on whether that surface is a free surface or a connected surface. A free surface experiences convection heat transfer to the ambient temperature. A connected surface experiences conduction heat transfer to the surface connected to it.

The convection resistance is given by

$$R_{conv} = \frac{1}{hA_s}, \tag{2}$$

where h is the convection heat transfer coefficient, and A_s is the surface area from which the heat is being lost to the ambient environment as shown in Fig.2. The thermal capacitance is given by

$$C = \rho\, c\, \mathrm{V}, \tag{3}$$

where ρ is the density of the material, c is the specific heat capacity of the material, and V is the volume of the corresponding element of the system.

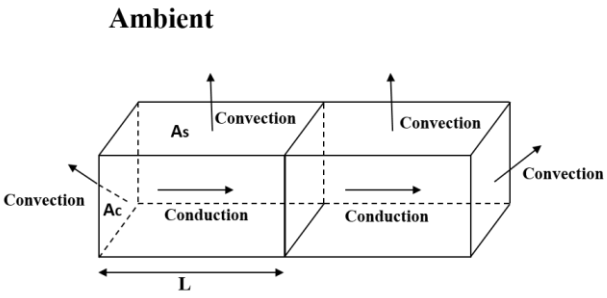

Fig.2. Types of heat transfer from 2 functional blocks

If the system is composed of multiple layers of different materials, it is convenient to treat the multilayered structure as a homogeneous material with an in-plane effective thermal conductivity given by

$$K_{in-plane} = \frac{\sum_{i=1}^{N} K_i t_i}{\sum_{i=1}^{N} t_i}, \tag{4}$$

where K_i is the thermal conductivity of a specific layer, t_i is the thickness of the corresponding layer, and N is the total number of layers. The effective thermal capacitance of the

multilayered structure is the sum of the thermal capacitance (3) of each layer

$$C = \sum_{i=1}^{N} C_i \tag{5}$$

B. Network modeling

In order to design a filter that provides an accurate dynamic spatial thermal estimation of the system, a state space representation of the thermal model is needed [7]. The state space is derived from a directed weighted graph G = (V, E, W) that represents the interconnected RC thermal model, where V = {1, 2, … , n} denotes the set of vertices of a graph of n nodes, E denotes the set of edges that connect adjacent vertices, and W denotes the weights of the edges which represent the thermal resistance values between the nodes of the thermal model. The ambient temperature is modeled by a single node (n+1) with an infinite capacitance. Each vertex represents a capacitor in the RC model. Each directed weighted edge represents the thermal resistance between two nodes in the RC model. The direction of the edge represents the direction of positive heat flow between the corresponding adjacent nodes. The resistance values of the edges are equal in both directions, i.e. $R_{ij} = R_{ji}$ on the edge (i,j). However, since the heat can flow only in one direction (from the higher temperature node to the lower temperature node), a direction was assigned to every node in the graph. This makes the graph directed. Fig.3 shows the graph-based model representation of the 2-D RC thermal model of Fig.1.

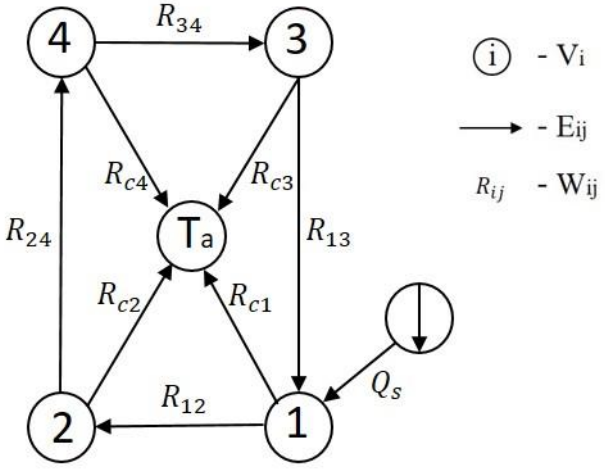

Fig.3. Example of a graph-based thermal model

The dynamic thermal behavior is then obtained by applying the conservation of energy law on every vertex in the graph-based model. The energy balance equation states that the thermal energy stored in each node is a function of the thermal energy entering the node, the thermal energy leaving the node, and the thermal energy generated in that node. This is given by

$$C_i \frac{dT_i}{dt} = q_i + Q_s - \frac{1}{R_{ci}}[T_i - T_a], \tag{6}$$

where C_i denotes the thermal capacitance at node i, T_i denotes the temperature of the node i, q_i denotes the net heat flow into node i from the adjacent nodes, and Q_s denotes the heat input from the current source connected to node i. The last term of the right hand side of the equation represents the convective heat transfer from node i to the ambient temperature, T_a denotes the ambient temperature, and R_{ci} denotes the convective heat transfer resistor of node i. It should be noted that heat generation is not present in all the nodes of the system. Hence, not all the nodes of system will have the Q_s term in their corresponding conservation of energy equation. The net heat flow into node i is obtained by adding the heat entering to the node and subtracting the heat leaving from the node. The heat flow from node j to node i is given by $(T_j - T_i)/ R_{ji}$. The set of the coupled differential equation can be expressed in a state space form as

$$\dot{\vec{x}} = A\vec{x} + B\vec{u} + V\vec{d}, \tag{7}$$

where the state vector $\vec{x}$ represents the temperature of each node or vertex of the graph, the matrix $A = [a_{ij}]$ represents the system dynamics, the vector $\vec{u}$ represents the heat input from the heat generating components in the system, and $\vec{d}$ represents the disturbance to the system which is the ambient temperature in this case. The system dynamics matrix is given by

$$a_{ij} = \begin{cases} 0, & i \neq j \quad (i,j) \notin E \\ \dfrac{1}{C_i R_{ij}}, & i \neq j \quad (i,j) \in E \\ -\displaystyle\sum_{k \neq i} a_{ik} - \frac{1}{C_i R_{ci}}, & i = j \quad (i,j) \in E \end{cases} \tag{8}$$

The resulting state space model of an actual physical system might have a large number of states which imposes high computational cost. Also, it will be problematic to implement such a complex system for online estimation. Therefore, a method that reduces the complexity of the system while preserving its accuracy is needed.

III. Model Order Reduction

The reduction in the complexity of the system is useful to reduce the simulation time of the model, the memory capacity needed, and the measurement data needed to find the parameters of the model. Also, it is highly desirable for on-line estimation purposes. There are many methods available in the field of model order reduction. The best known methods are Truncated Balanced Realization [15], Hankel-norm reduction [16], and Proper Orthogonal Decomposition [17]. For reducing the complexity of the RC thermal models studied in this paper, a model order reduction technique that preserves the physical intuition of the original RC thermal model is needed. Therefore, each node of the reduced order model needs to represent a specific location in the physical system. This physical correspondence between the thermal model and the physical system is needed for sensor placement.

The model order reduction technique used in this paper reduces the number of nodes of the thermal model while preserving its input output behavior and the correspondence with the physical system. This technique is an aggregation based approach developed in [18]. It provides a way to aggregate the nodes of the full order thermal model into single nodes, called "super-nodes", in the reduced order thermal model by applying the aggregation method of a continuous time Markov chain. The main idea behind this model order reduction technique is to find an optimal partition function $\varphi: V \to M$, where $M = \{1, 2, \ldots, m\}$ with $m < n$. The partition φ reduces the dimension of the state space from n nodes in the full order model into m nodes in the reduced order model, where m is specified by the user. Each super node has a super capacitance $\overline{C}$ and a super temperature $\overline{T}$. Super nodes are connected by super resistances $\overline{R}$. The super capacitance and the super- resistance are given by

$$\bar{C}_k = \sum_{i \in V} C_i, \tag{9}$$

$$\bar{R}_{kl} = \frac{1}{\sum_{i,j \in E} R_{ij}}. \tag{10}$$

In order to aggregate the nodes of the full order model, the optimal partition function φ has to be found. This function is difficult to get exactly when the order of the reduced order model is greater than 2 which is the general case in these applications. Instead, the reduced order model is obtained by applying a spectral algorithm on the symmetric matrix $\breve{P} = 0.5\,(\Delta^{\frac{1}{2}} P \Delta^{-\frac{1}{2}} + \Delta^{-\frac{1}{2}} P^T \Delta^{\frac{1}{2}})$ on the graph based model designed in Section II, with Δ = diag (π), where π is the stationary distribution of the Markov chain, and $P(t)$ is the Markov transition matrix. For the linear systems of interest (7), $P(t)$ is given by $P(t) := e^{At}$ [19]. The stationary distribution is given in terms of the capacitances by

$$\pi_i = \frac{C_i}{\sum_{j \epsilon V} C_j}, i \epsilon v. \tag{11}$$

The spectral algorithm steps used to obtain the reduced order thermal model are shown in Fig.4.

Algorithm

1. Construct $\breve{P}$: $\breve{P} = 0.5\left(\Delta^{\frac{1}{2}} P\, \Delta^{-\frac{1}{2}} + \Delta^{-\frac{1}{2}} P^T \Delta^{\frac{1}{2}}\right)$.
2. Check the sign of the second largest eigenvector of $\breve{P}$.
3. Aggregate the spatially adjacent nodes that share the same sign into super-nodes.
4. Calculate the super-capacitances and super-resistances (Neglect the internal resistances in the super-nodes).
5. Add the heat sources that exist in the same super-node into a single super-heat source.

Fig.4. Computation steps of the reduced order model

IV. Estimator Design

The final step in the temperature estimation of the thermally aware power electronic systems is to design an estimator that generates an accurate dynamic temperature distribution for the reduced order thermal model using the smallest possible number of sensors placed at the most efficient locations. The optimal estimator for the linear system (7) in the case of white noise is the well-known Kalman filter [9] [20] [21]. A Kalman filter was designed for the linear continuous time plant (7) and discrete time observations given by

$$y(m) = Hx(m) + v(m), \tag{12}$$

where $y(m)$ is the sensors output, H is a mapping from the true states into the observed states, and $v \sim$ N (0, R_k) is the measurement noise which is assumed to be white noise with zero mean and covariance R_k. In a continuous-discrete Kalman filter intermittent observations are easy to handle. The measurements from the temperature sensors can be taken at irregularly spaced instants of time. Another advantage of the continuous-discrete Kalman filter is that this approach provides the optimal state estimates continuously, including between the observations [21].

The computational cycle of the sequential estimation process of a continuous-discrete Kalman filter is shown in Fig.5. The a priori state estimate $\hat{x}_m^-$ is obtained by propagating $\hat{x}_{m-1}^+$through the state transition matrix $\emptyset(tm-1, tm)$, where the state transition matrix is defined by $d\emptyset(t,\tau)/dt = A\emptyset(t,\tau)$[21]. The a posteriori $\hat{x}_m^+$ is then obtained by updating $\hat{x}_m^-$ by the observations at time T_m.The recursive updating procedure is given by

$$\hat{x}_m^+ = \hat{x}_m^- + K_m(y(m) - H\hat{x}_m^-). \tag{13}$$

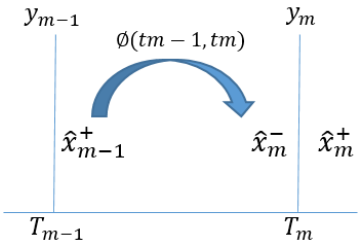

Fig.5. Graphical illustration of the continuous-discrete Kalman filter

The Kalman gain matrix K_m that results in the minimum variance estimate is given by

$$K_m = P_m^- H^T [H P_m^- H^T + R_m]^{-1}, \tag{14}$$

where the error covariance matrix $P_m^-$is the solution of

$$\dot{P} = AP + PA^T + Buu^T B^T. \tag{15}$$

V. Case Study

The thermal estimation technique developed in this article was applied to the multilevel DC-AC converter [22] shown in Fig.6. The main components of the circuit are GaN gate drivers, GaN transistors, ceramic capacitors, and Adum5210 digital isolators with integrated dc-to-dc converters.

The main printed circuit board (PCB) is composed of four layers of copper, three layers of FR4, and two solder mask layers. The daughterboard is composed of two copper layers, one FR4 layer, and two solder mask layers. The heat conduction problem was solved as a 2D problem. The board was divided into 39 elements, where each functional component of the board was assigned a capacitor value in the

2D RC thermal model. Since the PCB studied is multilayered, the in-plane effective thermal conductivity (4) and the effective heat capacitances (5) were used for the calculation of the R and C values of the thermal model. The board was tested for step loads of 800W. At this power level only the GaN transistors generated a significant amount of heat. The 12 transistors shown in Fig. 6 were modeled as current sources in the thermal network. The resulting 39 states thermal model was aggregated into 9 "super nodes." Fig. 7 shows the network of the 39 states full order model and the 9 super-nodes of the aggregated model.

The reduced order model was within an error of less than 3ºC with respect to the full order model. Fig. 8 shows the error between the fifth (tr_5) and sixth (tr_6) states of the reduced order model and their equivalent states of the full order model. The full order model states are represented by solid lines and the reduced order model states are represented by circles. IR thermal video was used for experimental validation using a FLIR T420 IR camera. Fig. 9 represents a snapshot from the thermal video at 2 minutes and 58 seconds after the voltage was applied to the converter. The temperature scale is in ºC. Fig. 10 shows the theoretical results vs the experimental results of the fifth and sixth states of the reduced order model. Experimental results are within an error of +/- 5ºC. The remaining states were not shown for brevity.

An optimization process with respect to the number of temperature sensors was performed. The optimization formulation has been done with the underlying assumption that there be can a maximum of 1 sensor per each state. It means that a particular state may either have a sensor or not. Therefore, it is a binary condition. Sensors can be placed based on the measures of degrees of Observability of states of dynamic systems. There are many such metrics by which one can determine the degree of observability of the states of a dynamic system [23]–[25]. The trace analysis of the Observability Gramian [26], [27] has been considered as the performance metric for this application. The larger the trace of the observability Gramian, the greater is the observability of such a kind of sensor placement.

There are 2^9 and 2^{39} combinations in which the temperature sensors can be placed for the reduced order model and full order model, respectively.

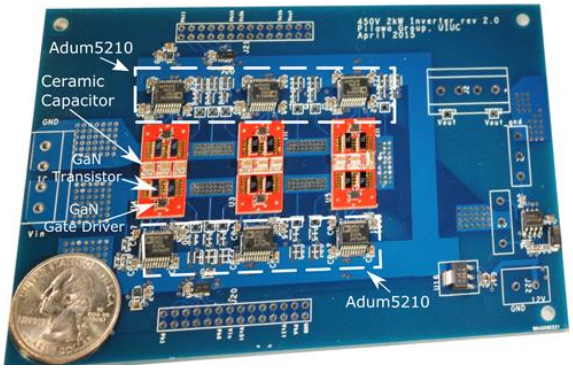

Fig.6. Multilevel DC-AC Converter

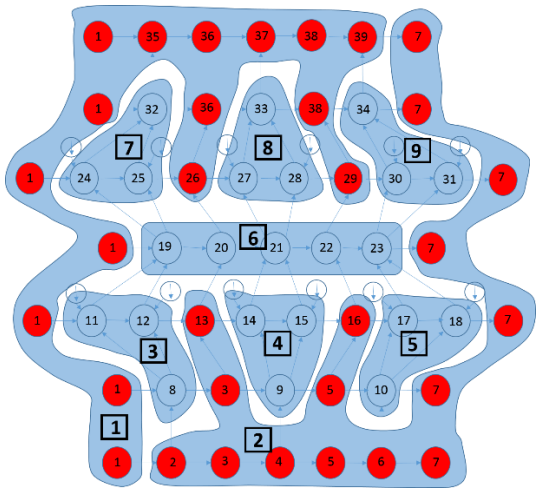

Fig.7. Directed weighted graph representing the interconnected RC thermal model of the full order model and the reduced order model

As the number of sensors increases, the trace of the Observability Gramian increases. Hence, there exists a trade-off between the degree of observability and number of sensors that can placed on the PCB. The optimization has been performed using Genetic Algorithm (GA) Mixed Integer programming since the decision variable is an integer which can take a value of either one or zero. The optimal number of temperature sensors was 5 sensors. The optimal number of sensors was decided by taking into account the states estimation error when using the corresponding number of sensors in the Kalman filter. The optimal locations of the 5 sensors, according to the metric used, were on super nodes 1, 2, 5, 6, and 7. A Kalman filter was designed for the reduced order model. Numerical values of the filter parameters are shown in the Appendix. Fig. 11 shows the theoretical versus the estimated values of the fifth and sixth states of the reduced order model respectively.

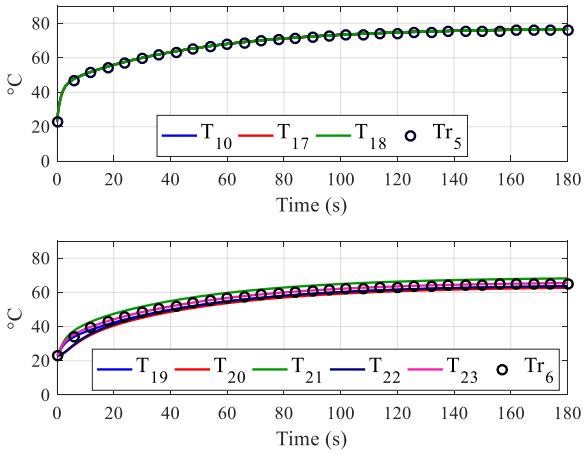

Fig.8. Fifth and sixth state of the reduced order model vs equivalent states of the full order model obtained from the RC model

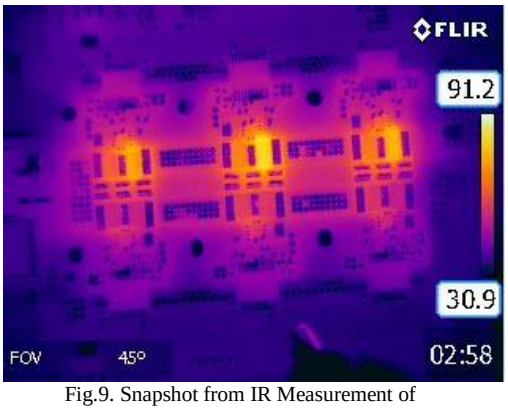

Fig.9. Snapshot from IR Measurement of Operating Multilevel Inverter

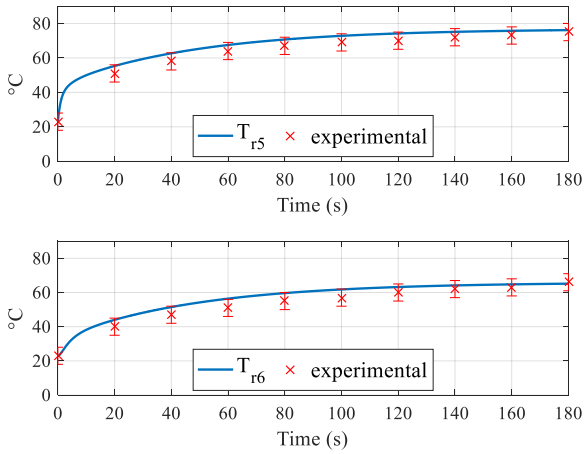

Fig.10. Theoretical results (RC model) vs experimental results (IR thermal video) of the fifth and sixth states of the reduced order model.

The states of the full order model were also estimated by applying a reduced order Kalman filter on the full order model. Since there is a small error between the states of the full order model and the states of the reduced order model, the estimated values of the states of the full order model were slightly different than the theoretical values of these states.

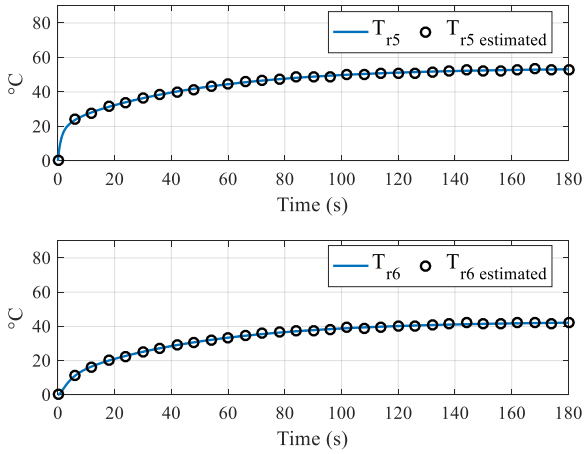

Fig.11. Theoretical (RC model) vs estimated (Kalman filter) values of the fifth and sixth states of the reduced order model

However, the estimation errors were still less than 3ºC. Fig.12 shows the estimated values of the fifth and sixth states of the reduced order model obtained from the Kalman filter versus their corresponding theoretical equivalent states in the full order model obtained from the full order RC model.

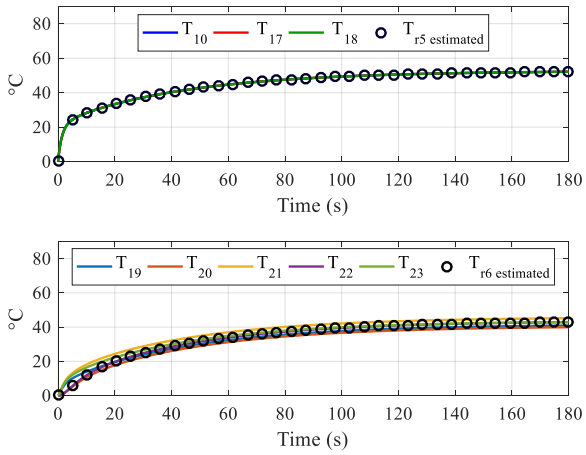

Fig.12. Estimated values of the fifth and sixth states of the reduced order model (Kalman filter) vs their corresponding theoretical equivalent states in the full order model (RC model)

VI. Conclusion

Accurate state estimates are essential for dynamic thermal management techniques and high power density systems. This paper provides a set of tools that can be used for temperature estimation of highly complex and interconnected thermal systems. The dynamic spatial temperature profile of lumped parameter models was accurately reconstructed using an optimal estimator together with an optimal number and placement of temperature sensors. A structure-preserving model order reduction technique based on Markov chain aggregation was used to reduce the complexity of the thermal model. The reduced order model was within an error of less than 3ºC with respect to the full order model. The states of the reduced order model were estimated with an estimation error of less than 1ºC using 5 temperature sensors. A reduced order estimator was also applied to the full order thermal model. The states of the high dimensional model were estimated using the same number of temperature sensors with an estimation error of less than 3ºC.

APPENDIX

Kalman filter parameters for the reduced order model:

$$A = \begin{bmatrix} -0.28 & 0.22 & 0.01 & 0.00 & 0.00 & 0.01 & 0.02 & 0.01 & 0.01 \\ 0.22 & -0.28 & 0.01 & 0.01 & 0.02 & 0.01 & 0.00 & 0.00 & 0.01 \\ 0.25 & 0.21 & -0.94 & 0.00 & 0.00 & 0.39 & 0.00 & 0.00 & 0.00 \\ 0.00 & 0.33 & 0.00 & -0.81 & 0.00 & 0.39 & 0.00 & 0.00 & 0.00 \\ 0.00 & 0.46 & 0.00 & 0.00 & -0.94 & 0.39 & 0.00 & 0.00 & 0.00 \\ 0.03 & 0.03 & 0.07 & 0.07 & 0.07 & -0.5 & 0.07 & 0.07 & 0.07 \\ 0.46 & 0.00 & 0.00 & 0.00 & 0.00 & 0.39 & -0.94 & 0.00 & 0.00 \\ 0.33 & 0.00 & 0.00 & 0.00 & 0.00 & 0.39 & 0.00 & -0.81 & 0.00 \\ 0.21 & 0.25 & 0.00 & 0.00 & 0.00 & 0.39 & 0.00 & 0.00 & -0.94 \end{bmatrix}$$

$$B = \begin{bmatrix} 0 & 0 & 0 & 0 & 0 & 0 \\ 0 & 0 & 0 & 0 & 0 & 0 \\ 12.5 & 0 & 0 & 0 & 0 & 0 \\ 0 & 12.5 & 0 & 0 & 0 & 0 \\ 0 & 0 & 12.5 & 0 & 0 & 0 \\ 0 & 0 & 0 & 0 & 0 & 0 \\ 0 & 0 & 0 & 12.5 & 0 & 0 \\ 0 & 0 & 0 & 0 & 12.5 & 0 \\ 0 & 0 & 0 & 0 & 0 & 12.5 \end{bmatrix}$$

$$u = \begin{bmatrix} 1.2 & 1.5 & 1.4 & 0.16 & 0.2 & 0.16 \end{bmatrix}$$

$$K_m = \begin{bmatrix} 0.67 & 0.33 & 0.00 & -0.05 & 0.05 \\ 0.33 & 0.66 & 0.00 & 0.05 & -0.05 \\ 0.11 & -0.08 & 0.84 & 0.00 & 0.12 \\ -0.28 & 0.48 & 1.18 & 0.56 & -0.99 \\ 0.00 & 0.00 & 1.00 & 0.00 & 0.00 \\ -0.05 & 0.05 & 0.00 & 0.99 & 0.01 \\ 0.05 & -0.05 & 0.00 & 0.01 & 0.99 \\ 0.21 & -0.35 & 0.03 & 0.10 & 1.02 \\ -0.10 & 0.06 & -0.01 & 0.01 & 1.05 \end{bmatrix}$$

REFERENCES

[1] M. Pedram and S. Nazarian, "Thermal Modeling, Analysis, and Management in VLSI Circuits: Principles and Methods," *Proc. IEEE*, vol. 94, no. 8, pp. 1487–1501, 2006.

[2] W. Huang, S. Ghosh, S. Velusamy, K. Sankaranarayanan, K. Skadron, and M. R. Stan, "HotSpot: A compact thermal modeling methodology for early-stage VLSI design," *IEEE Trans. Very Large Scale Integr. Syst.*, vol. 14, no. 5, pp. 501–513, 2006.

[3] A. K. Coskun, T. S. Rosing, and K. Whisnant, "Temperature aware task scheduling in MPSoCs," *Proc. -Design, Autom. Test Eur. DATE*, pp. 1659–1664, 2007.

[4] F. Zanini, D. Atienza, C. N. Jones, and G. De Micheli, "Temperature sensor placement in thermal management systems for MPSoCs," *Circuits Syst. (ISCAS), Proc. 2010 IEEE Int. Symp.*, pp. 1065–1068, 2010.

[5] C. H. Lim, W. R. Daasch, and G. Cai, "A thermal-aware superscalar microprocessor," *Proc. - Int. Symp. Qual. Electron. Des. ISQED*, vol. 2002–Janua, pp. 517–522, 2002.

[6] M. Iachello, G. S. Member, V. De Luca, G. Petrone, N. Testa, L. Fortuna, G. Cammarata, and S. Graziani, "Lumped Parameter Modeling for Thermal Characterization of High-Power Modules," vol. 4, no. 10, pp. 1613–1623, 2014.

[7] S. Sharifi and T. S. Rosing, "Accurate Direct and Indirect On-Chip Temperature Sensing for Efficient Dynamic Thermal Management," *IEEE Trans. Comput. Des. Integr. Circuits Syst.*, vol. 29, no. 10, pp. 1586–1599, 2010.

[8] Y. Zhang, A. Srivastava, and M. Zahran, "Chip level thermal profile estimation using On-chip temperature sensors," *26th IEEE Int. Conf. Comput. Des. 2008, ICCD*, no. 1, pp. 432–437, 2008.

[9] Y. Zhang and A. Srivastava, "Adaptive and autonomous thermal tracking for high performance computing systems," *Proc. 47th Des. Autom. Conf. - DAC '10*, p. 68, 2010.

[10] Derek P.Atherton, *Nonlinear Control Engineering*. Van Nostrand Reinhold, 1982.

[11] S. Sharifi, C. C. Liu, and T. S. Rosing, "Accurate temperature estimation for efficient thermal management," *Proc. 9th Int. Symp. Qual. Electron. Des. ISQED 2008*, pp. 137–142, 2008.

[12] G. Swift, T. S. Molinski, and W. Lehn, "A fundamental approach to transformer thermal modeling - Part I: Theory and equivalent circuit," *IEEE Trans. Power Deliv.*, vol. 16, no. 2, pp. 171–175, 2001.

[13] K. Skadron, T. Abdelzaher, and M. R. Stan, "Control-theoretic techniques and thermal-RC modeling for accurate and localized dynamic thermal management," *Proc. Eighth Int. Symp. High Perform. Comput. Archit.*, 2002.

[14] C. Jena, N. Sarbhai, R. Mulaveesala, and S. Tuli, "Pulsed Thermography Simulation : 1D , 2D and 3D Electro-Thermal Model Based Evaluation," *Simulation*, no. 1, 2006.

[15] B. Moore, "Principal component analysis in linear systems: Controllability, observability, and model reduction," *IEEE Trans. Automat. Contr.*, vol. 26, no. 1, pp. 17–32, 1981.

[16] K. Glover, "All optimal Hankel-norm approximations of linear multivariable systems and their L, ∞ -error bounds," *Int. J. Control*, vol. 39, no. 6, pp. 1115–1193, 1984.

[17] W. Schilders, "Introduction to Model Order Reduction," *Model order Reduct. theory, reasearch Asp. Appl.*, 2008.

[18] K. Deng, P. Barooah, P. G. Mehta, and S. P. Meyn, "Building Thermal Model Reduction via Aggregation of States," *Am. Control Conf.*, pp. 5118–5123, 2010.

[19] K. Deng, S. Goyal, P. Barooah, and P. G. Mehta, "Structure-preserving model reduction of nonlinear building thermal models," *Automatica*, vol. 50, no. 4, pp. 1188–1195, 2014.

[20] V. Tzoumas, A. Jadbabaie, and G. J. Pappas, "Sensor Placement for Optimal Kalman Filtering: Fundamental Limits, Submodularity, and Algorithms," pp. 191–196, 2015.

[21] P. D. B. Kovacevic and P. D. Z. Durovic, *Fundamentals of Stochastic Signals, Systems and Estimation Theory with Worked Examples*, Second. 2008.

[22] Y. Lei, C. Barth, S. Qin, W.-C. Liu, I. Moon, S. Andrew, D. Chou, T. Foulkes, Z. Ye, Z. Liao, and R. C. N. Pilawa-Podgurski, "A 2 kW, Single-Phase, 7-Level, GaN Inverter with an Active Energy Buffer Achieving 216 W/in3 Power Density and 97.6% Peak Efficiency," *2016 IEEE Appl. Power Electron. Conf. Expo. - APEC 2016*, pp. 1512–1519, 2016.

[23] A. K. Singh and J. Hahn, "Determining Optimal Sensor Locations for State and Parameter Estimation for Stable Nonlinear Systems," *Ind. Eng. Chem. Res.*, vol. 44, no. 15, pp. 5645–5659, 2005.

[24] A. K. Singh and J. Hahn, "On the use of empirical gramians for controllability and observability analysis," pp. 140–146, 2005.

[25] J. Brewer, Z. Huang, A. K. Singh, M. Misra, and J. Hahn, "Sensor Network Design via Observability Analysis and Principal Component Analysis," *Ind. Eng. Chem. Res.*, vol. 46, pp. 8026–8032, 2007.

[26] F. Zanini, D. Atienza, and G. De Micheli, "A combined sensor placement and convex optimization approach for thermal management in 3D-MPSoC with liquid cooling," *Integr. VLSI J.*, vol. 46, no. 1, pp. 33–43, 2013.

[27] N. A. Samad, J. B. Siegel, A. G. Stefanopoulou, and A. Knobloch, "Observability analysis for surface sensor location in encased battery cells," *Proc. Am. Control Conf.*, vol. 2015–July, pp. 299–304, 2015.